International Journal of Mining Science and Technology 27 (2017) 57–64

Contents lists available at ScienceDirect

International Journal of Mining Science and Technology

journal homepage: www.elsevier.com/locate/ijmst

Assessment of potential impacts to surface and subsurface water bodies due to longwall mining

Christopher Newman, Zacharias Agioutantis *, Gabriel Boede Jimenez Leon

Department of Mining Engineering, University of Kentucky, Lexington, KY 40506, USA

ARTICLE INFO

Article history:
Available online 29 December 2016

Keywords:
Streams
Aquifers
Ground strain
Coal mining

ABSTRACT

Ground movements due to longwall mining operations have the potential to damage the hydrological balance within as well as outside the mine permit area in the form of increased surface ponding and changes to hydrogeological properties. Recently, the Office of Surface Mining, Reclamation and Enforcement (OSMRE) in the USA, has completed a public comment period on a newly proposed rule for the protection of streams and groundwater from adverse impacts of surface and underground mining operations (80 FR 44435). With increased community and regulatory focus on mining operations and their potential to adversely affect streams and groundwater, now there is a greater need for better prediction of the possible effects mining has on both surface and subsurface bodies of water. With mining induced stress and strain within the overburden correlated to changes in the hydrogeological properties of rock and soil, this paper investigates the evaluation of the hydrogeological system within the vicinity of an underground mining operation based on strain values calculated through a surface deformation prediction model. Through accurate modeling of the pre- and post-mining hydrogeological system, industry personnel can better depict mining induced effects on surface and subsurface bodies of water aiding in the optimization of underground extraction sequences while maintaining the integrity of water resources.

1. Introduction

The utilization of high-recovery underground mining methods, such as longwall or high-extraction room-and-pillar operations, has the potential to cause adverse impacts to both surface and subsurface bodies of water as strata movement and deformations propagate from the mined seam through the overburden to the surface [1].

Previous research has indicated that mining induced strains are the most damaging to surface streams as well as greatly affecting the integrity of subsurface bodies of water and groundwater flow conditions [2,3]. On the surface, adverse effects to the stream can occur due to the development of either tensile or compressive strain in the stream bed. The development of tensile cracks along the bedrock allows for a potential loss of stream flow through developed fissures. The potential impact of longwall mining on the hydrogeological environment typically results in a drop in the groundwater table culminating in water loss to the surface by altering water flow paths [4]. In fact, water flow in the Cataract River of Australia ceased in 1994 as a result of mining-induced strains from longwall operations in the Bulli Seam 430 m below the river gorge [5]. On the other hand, the development of compressive strains within the rock layers can cause rupturing or buckling of the stream bed, blocking stream flow and/or diverting flow into the fractures at the base [6]. While these localized fractures can contribute to the loss of stream flows, given time, damaged streams have the ability to self-heal through the regeneration of near-surface aquifers as well as the sealing of mining-induced fractures with rock debris, gravel, sand, clay or other soil particles carried from upstream sources and deposited in the river bed [7].

Below the surface, mining-induced strains can initiate subsidence and fracturing of the strata, causing changes to the hydraulic conductivity and affecting flow paths within the overburden [8]. Recently, the Office of Surface Mining Reclamation and Enforcement (OSMRE) in the USA has completed the public comment period on a newly proposed rule for the protection of streams and groundwater from the adverse impacts of surface and underground mining operations (80 FR 44435). These proposed regulations call for an increase in baseline data collection, pre- and post-mining monitoring and mitigation/restoration practices, as well as increased focus on possible mining-induced damages to the hydro-

* Corresponding author.
E-mail address: zach.agioutantis@uky.edu (Z. Agioutantis).

http://dx.doi.org/10.1016/j.ijmst.2016.11.016
2095-2686/

geological balance within the mine permit area, which includes both surface and subsurface bodies of water. With an increase in environmental scrutiny from both local communities and regulatory agencies, this paper investigates the application of a numerical modeling approach for a more realistic evaluation of mining impacts to both surface and subsurface bodies of water.

Since the determination of the strain regime above an underground mine is integral to this investigation, the Surface Deformation Prediction Software (SDPS), a package developed at Virginia Tech, USA will be utilized to calculate mining-induced strains at different elevations above the seam as well as on the surface [9]. Surface strain calculations now include the effect of varying topography, while subsurface strain outputs from SDPS will be used to assess changes to the hydraulic conductivity of affected strata. An assessment of the post-mining hydrogeological system using a hypothetical case study will be presented through the application of MODFLOW, a groundwater modeling software package available through the United States Geologic Survey (USGS) [10].

This paper presents two conceptual case studies that demonstrate: (a) the effect of variable surface topography on ground strains in the vicinity of a linear surface body (e.g., a stream) and (b) the effect of horizontal strain magnitude in the overburden on the hydraulic conductivity of different formations potentially impacted by underground mining.

2. Background

2.1. Importance of strain in assessing potential impacts to the surface and subsurface

The influence function method, as implemented by SDPS, for the calculation of ground deformations is a mature methodology widely used by academic, industry and regulatory personnel [9]. Through the application of this Gaussian bell-shaped influence function in SDPS, one is able to calculate horizontal displacement as a linear function of the first derivative of subsidence and horizontal strain as the first derivative of horizontal displacement. Recent advances in the SDPS package allow for the calculation of directional strain and ground strain along a profile as well as ground strain for random prediction points by calculating the 3D distance between neighboring surface points [11,12]. The influence function formulation can accurately calculate deformations at any point in 3D space and, therefore, at any point on the surface and at any elevation between the seam and the surface. This is conceptually depicted in Fig. 1, where a typical horizontal strain distribution across a transverse profile line over a rectangular panels of 2 m extraction height at a depth of 150 m. Additionally, a horizontal strain curve is calculated within the overburden at depth equal to half the overburden height or 75 m. Although strain magnitudes increase as the distance from the extracted panel decreases, the inflection point of the strain curve remains above the rib.

These calculations can be easily utilized to determine potential surface impacts or used to derive other physical parameters for surface or groundwater modeling [13].

It should be emphasized, however, that further adjustments are necessary when these ground strain calculations or strain calculations within a given formation are applied to man-made structures in contact with the ground, such as buildings or pipelines [14].

2.2. Relating horizontal strain magnitudes to changes in hydraulic conductivity

While the majority of research has focused on mining-induced strain damages at the surface, strain magnitudes within the overburden can also cause detrimental impacts to the strata overlying a mined panel. Overburden strains discussed in this paper refer to the maximum horizontal strains developed within the geologic strata and, as already mentioned, can be calculated by SDPS at any point between the seam and the surface. Similar to the effects of increased strains at the surface, strains within the overburden can cause mining-induced fracturing of the overburden leading to the dewatering of both surface and subsurface bodies of water through the subsequent and large increase in hydraulic conductivity [15]. While academic and industry research acknowledges that changes to the hydraulic conductivity within the overburden material can alter the groundwater system, few studies have investigated the interaction between mining-induced strata deformations and the modifications to hydraulic conductivity [16–18].

In lieu of tedious and time-consuming groundwater monitoring regimes, groundwater flow models are often used to evaluate the impact of mining operations on the hydrogeological system through the prediction of groundwater flows and transportation processes. The three-dimensional finite-difference groundwater flow model, MODFLOW, provides users with a mathematical description of groundwater flows as well as surface-groundwater interaction through the application of Darcy's equation for fluid flow in porous material [10]. Distributed to users through the USGS web site, MODFLOW is widely used within the mining industry to simulate groundwater seepage into mine openings or shafts [19]. As with any numerical model, realistic model estimations are closely tied to input parameters; therefore, it is important that users have detailed information on site-specific geology, water quality, recharge, river locations, water levels, hydraulic parameters, etc., as well as a clear understanding of numerically embedded assumptions within the numerical modeling code such as boundary conditions, layer types, etc.

In order to accurately simulate groundwater flow paths, it is important that users can accurately quantify the hydraulic conductivity of the overburden strata material. Typically determined through borehole slug tests, hydraulic conductivity is the proportionality constant of Darcy's equations (K), which relates the amount of flow through a unit cross-sectional area (A) of an aquifer under a unit gradient of hydraulic head ($\Delta h/\Delta L$).

$$Q = KA\frac{\Delta h}{\Delta L} \tag{1}$$

In reviewing the literature, a wide range of pre- and post-mining hydraulic conductivities have been documented (as summarized in Table 1). These values have been determined through a series of in-situ borehole slug tests and/or back calculations from groundwater monitoring regimes. In reviewing the values presented in Table 1, all testing seems to indicate pre- and post-mining hydraulic conductivities within similar ranges. For shale materials in the overburden, the data suggests a pre-mining hydraulic conductivity in the order of 10^{-8} to 10^{-9} m/s with post-mining conductivities increasing by one or two orders of magnitude. For sandstone materials, the data suggests typical pre-mining hydraulic conductivity values ranging in the order of 10^{-4} to 10^{-5} m/s with post-mining conductivities again increasing by 10- or 100-fold. Limestone channels within the overburden material have pre-mining hydraulic conductivities ranging in the order of 10^{-8} to 10^{-10} m/s; post-mining hydraulic conductivity were not available.

While the majority of the literature reviewed points to the same range of pre- and post-mining hydraulic conductivity for overburden strata materials, the data published by Li et al. has significantly higher conductivities for all materials [21]. In further reviewing this publication, it is believed that the units may have been mislabeled (ft/day instead of m/s). Under this assumption, conductivity values collaborate well with the other published data. The change in hydraulic conductivity between pre- and post-mining activity is

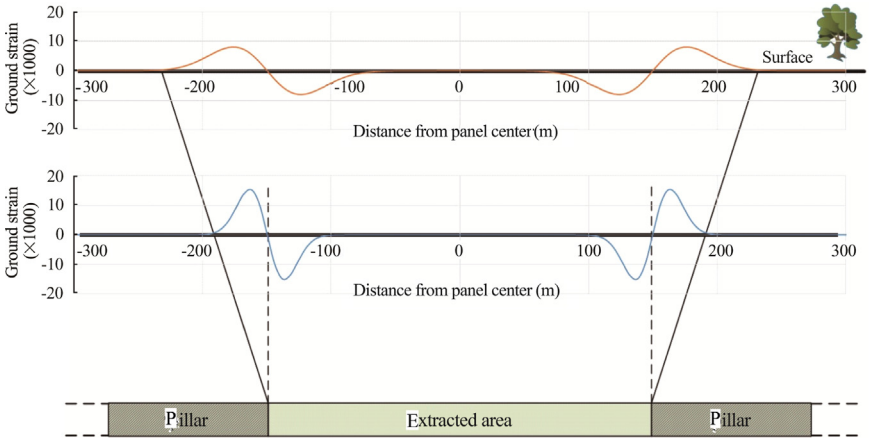

Fig. 1. Distribution of horizontal strains at and below the surface over an underground extraction area.

Table 1
Hydraulic conductivity values (m/s).

	Shale		Sandstone		Limestone	Coal seam		Aquifer	
	Pre-mining	Post-mining	Pre-mining	Post-mining	Pre-mining	Pre-mining	Post-mining	Post-mining	
Horizontal	7.01E−08 to 7.01E−09	7.01E−06 to 7.01E−08	7.01E−05	7.01E−03					Matetic et al. [20]
Vertical	7.01E−08 to 7.01E−09	7.01E−07 to 7.01E−08	7.01E−05	7.01E−04					Matetic et al. [20]
Horizontal	1.13E−07 to 9.53E−08	2.89E−05 to 3.53E−07	1.14E−06 to 4.23E−08	2.85E−05 to 3.42E−06	1.76E−09	1.76E−09			Li et al. [21]
Horizontal								1.65E−03 to 6.1E−06	Toran and Bradbury [22]
Vertical		6.1E−09 to 6.1E−11							Toran and Bradbury [22]
Horizontal							1.74E−06 to 3.47E−07		McCoy et al. [23]
Horizontal			1.0E−04 to 1.0E−05						Rapantova et al. [24]
Horizontal	8.89E−09 to 2.28E−09				1.09E−08 to 5.43E−10				Karacan and Goodman [8]

similar in magnitude change (10- to 100-fold), the data seems to suggest that there were previous impacts to the overlying strata causing such high pre-conductivity values.

According to the work of Ouyang and Elsworth, after determining the mining-induced strain field around a given panel, one can approximate the post-mining hydraulic conductivity of overburden material using the following equations [25]:

$$K_x = K_{xo} \times \left[1 + \frac{b + S(1 - R_m)}{b} \Delta\varepsilon_y\right]^3 \quad (2)$$

$$K_y = K_{yo} \times \left[1 + \frac{b + S(1 - R_m)}{b} \Delta\varepsilon_x\right]^3 \quad (3)$$

where K_x and K_y are the post-mining hydraulic conductivities in the horizontal and vertical directions determined as a function of the pre-mining conductivity in the horizontal and vertical directions (K_{xo} and K_{yo}), the fracture aperture (b) and spacing (S), a modulus reduction ratio (R_m), and the mining-induced strains in the horizontal ($\Delta\varepsilon_x$) and vertical ($\Delta\varepsilon_y$) directions.

Thus, using the predicted, calculated, and/or measured mining-induced strains within the overburden strata, one is able to approximate the post-mining hydraulic conductivity. Table 2 was generated using assumed values for the geometric parameters S (0.33 m), b (1 mm or 0.001 m) and R_m (0.8) of Eq. (3). Post-mining hydraulic conductivity increases as the strain magnitude increases by a factor of 1.2 for a strain value of 1 mm/m to a factor of 82.3 for a strain value of 50 mm/m.

Following the determination of changes in hydraulic conductivity with respect to mining-induced strains, the post-mining hydrogeological system may subsequently be defined through the application of a groundwater model [15].

A summary of the steps required are shown in the brief flowchart depicted in Fig. 2. Users can input mine and surface geometry and overburden parameters into the influence function method of the SDPS package and calculate strain at any point within the overburden with respect to the defined mine layout. Taking the horizontal strain outputs from SDPS and averaging them over specific regions, one can then estimate the post-mining hydraulic conductivity with respect to Eq. (3). Finally, by implementing the post-mining hydraulic conductivity values as input parameters to a hydrogeological model, one can effectively approximate the changes in groundwater flow with respect to mining-induced strains in the overburden.

2.3. Conceptual case studies

2.3.1. Case study 1: the effect of variable topography on ground strains in the vicinity of a linear water body

To highlight the differences in the horizontal and ground strain calculations, the following case study was developed in SDPS to evaluate strain magnitudes with respect to stream location, stream orientation, and topographic relief. For each scenario presented in

Table 2
Approximation of vertical post-mining hydraulic conductivity with respect to mining-induced horizontal strain based on the formulation by Ouyang and Elsworth [25].

ε_x	S	b (m)	R_m	K_{yo}		K_y		K_y/K_{yo}
				(m/s)	(m/day)	(m/s)	(m/day)	
0.001	0.33	0.001	0.8	5.00E−08	4.32E−03	6.07E−08	5.25E−03	1.2
0.010	0.33	0.001	0.8	5.00E−08	4.32E−03	2.33E−07	2.01E−02	4.7
0.020	0.33	0.001	0.8	5.00E−08	4.32E−03	6.41E−07	5.54E−02	12.8
0.050	0.33	0.001	0.8	5.00E−08	4.32E−03	4.12E−06	3.56E−01	82.3

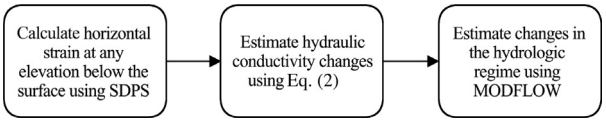

Fig. 2. Flow chart for the approximation of groundwater flow with respect to mining-induced strains in the overburden material.

case study 1 a stream was defined within the vicinity of or overlying a longwall panel at a depth of 150 m, extraction thickness of 2 m, supercritical subsidence factor of 50%, and an edge effect of 0 m. Default parameters were assigned by the SDPS program for defining the ground response. A discussion regarding the difference between horizontal and ground strains is available in Agioutantis and Karmis and also in Agioutantis et al. [11,13]. Positive horizontal or ground strain values correspond to tension, while negative strain values correspond to compression.

In Scenario 1a, horizontal and ground strains were calculated along a transverse line (stream) which bisects the longwall across the full extent of the subsidence trough without any subsidence influence from either end of the panel. Prediction points were defined along a transverse line as shown in Fig. 3. From the results of Scenario 1a, one finds similar horizontal strain (Em) and ground strain (EGA) profiles with the ground strain calculation having slightly lower magnitudes for the peak compressive and tensile strains. These differences in the strain profiles are attributed to the integration of the total displacement from pre- and post-mining surface elevations.

In Scenario 1b horizontal and ground strains were determined along a stream which again, was defined such that it bisects the longwall panel across the full extent of the subsidence trough. Prediction points for Scenario 1b were defined such that the stream dips at a 5° angle from west to east (Fig. 4). Given the sloping terrain, there is an overall strain increase on the downhill side of the stream and an overall strain decrease on the uphill side. As previously stated in Scenario 1a, differences in the strain profiles are due

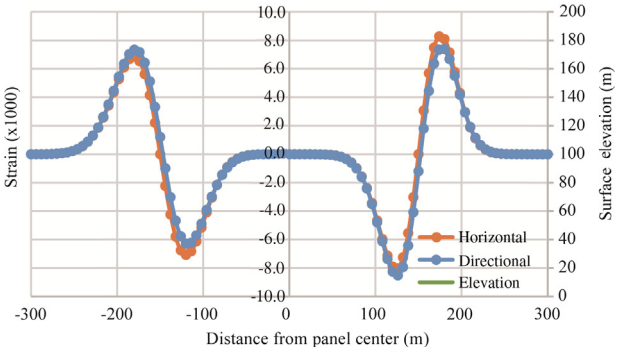

Fig. 4. Case 1 Scenario 1b–transverse profile, surface sloped at 5 degrees.

to the incorporation of the pre- and post-mining surface elevations. From these results, one finds that the ground strain calculation provides lower strains in the tensile downhill region and compressive uphill regions of the subsidence trough in comparison to the horizontal strain calculation.

In Scenarios 1c and 1d horizontal and ground strains were determined along a stream, which crosses the full extent of the subsidence trough at a 45° angle (Fig. 5). The prediction points for Scenario 1c were defined along a flat lying horizontal plane. From the results of Scenario 1c, one finds that the maximum horizontal strain magnitude is much larger than that determined by the ground strain calculation. By evaluating strain magnitudes with respect to the change in pre- and post-mining surface elevations as well as the directional strain vectors between consecutive points along the stream path, the ground strain calculation provides a more accurate depiction of the strain developed along the defined stream bed.

In Scenario 1d prediction points were redefined such that the stream dips at a 5° angle from west to east crossing the subsidence trough at a 45° angle (Fig. 6). From the results of Scenario 1d one

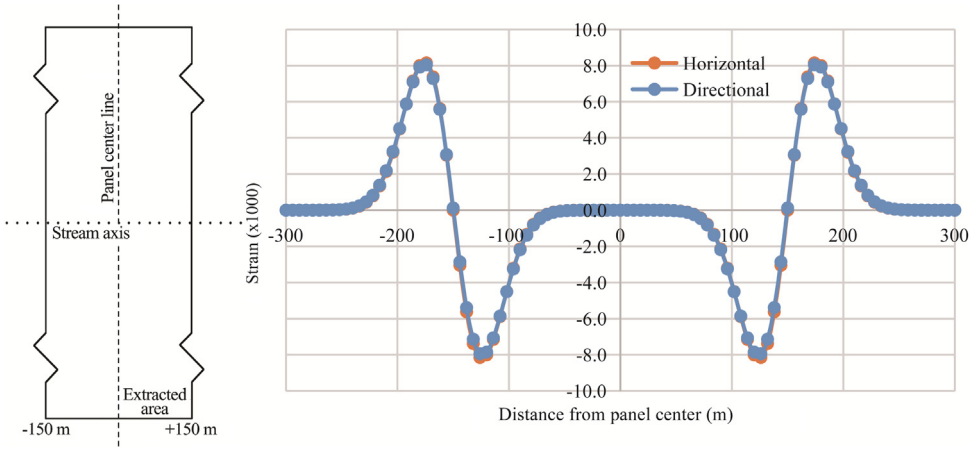

Fig. 3. Case 1 Scenario 1a–transverse profile, flat lying stream.

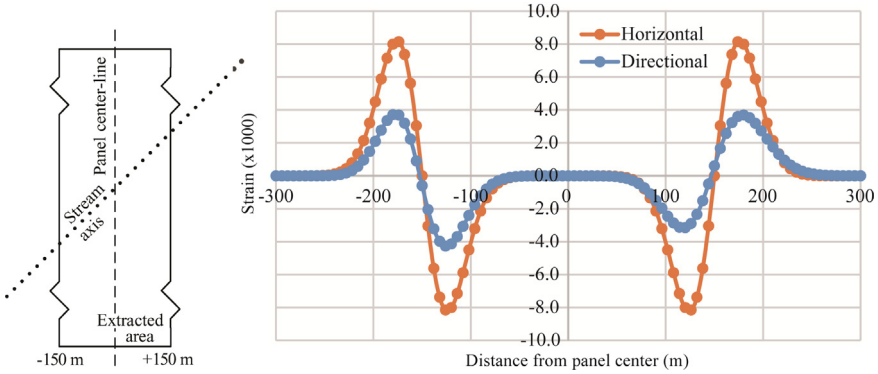

Fig. 5. Case 1 Scenario 1c–angled profile, flat lying stream.

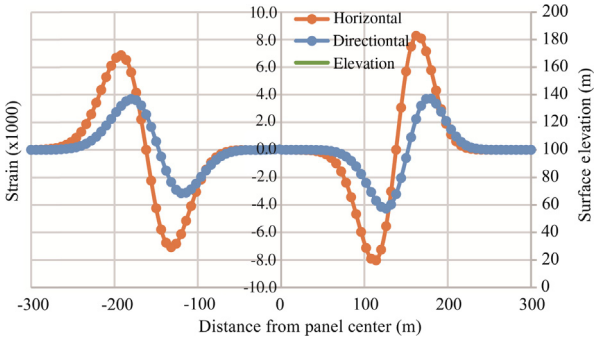

Fig. 6. Case 1 Scenario 1d–angled profile, surface sloped at 5 degrees.

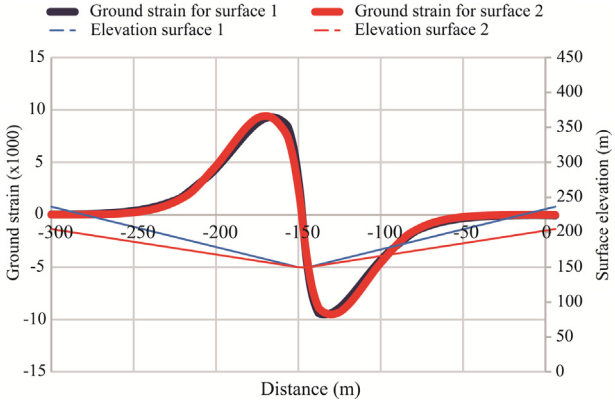

Fig. 8. Ground strain profiles on a transverse line above a longwall panel with respect to varying topography.

finds, through the incorporation of changes to the pre- and post-mining surface elevations and directional strain values, that the ground strain calculation determines strain magnitudes which are significantly less than that of the horizontal strain magnitudes in the maximum compression and tensile zones providing a more realistic evaluation of the strain developments along the stream bed.

Scenario 1e through Scenario 1k further investigate the effect of varying topography over and in the vicinity of the high extraction area. The geometry of the extracted longwall panel and the transverse prediction line are shown in Fig. 7a. The elevation profile presented in Fig. 7b simulates a stream flowing at the bottom of a valley along the longitudinal axis of a longwall panel. Starting from the west side of the panel, elevations gradually decrease to a minimum point that represents the stream bed and then increase again towards the eastern side of the panel.

Fig. 8 shows the distribution of strain along the transverse profile shown in Fig. 7b. Positive horizontal or ground strain values correspond to tension, and negative strain corresponds to compression. Two ground strain profiles are plotted: one corresponds to a surface inclination of 20°, and the other to a surface inclination of 30°. Ground strain magnitudes are comparable for both profiles.

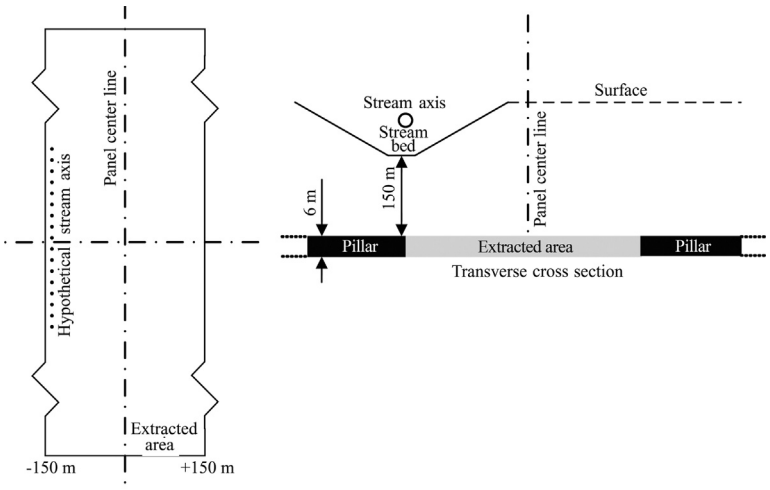

(a) Plan view of modeled area (b) Section view of modeled area

Fig. 7. Case 1 Scenario 1e–1k geometry and location information.

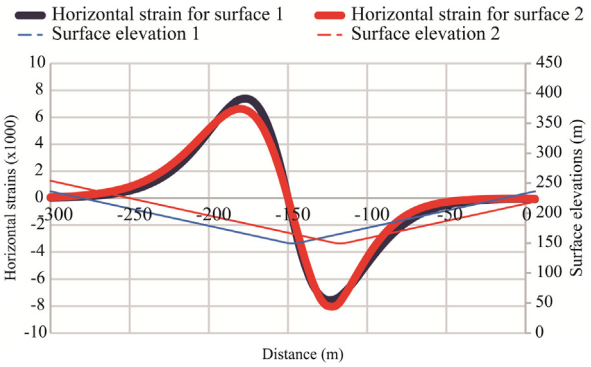

Fig. 9. Horizontal strain profiles on a transverse line above a longwall panel.

The zero strain point has slightly moved inby due to the ground strain adjustment.

As shown in Fig. 8, surface 1 corresponds to 30° and Surface 2 to 20°.

Fig. 9 presents the distribution of horizontal strain along two similar transverse profiles that differ only with respect to the horizontal location of the minimum elevation area. Strain magnitudes are again similar, and the slight differences can be attributed to the elevation differences between the two curves.

As noted in Fig. 9, surfaces 1 and 2 are both sloping 30° to the horizontal, but with a different location of the minimum elevation.

Fig. 10 shows the distribution of ground strain along three transverse profiles; the difference between the profiles is the location of the stream bed with respect to the rib of the extracted area. The inflection point of the ground strain curve is displaced with respect to the rib, depending on the surface curve. Ground strain magnitudes are similar although the shape of the peak tensile regime and peak compressive regime may differ.

As is evident in Fig. 10, the stream bed in surface 1 is close to the rib, the stream bed in surface 2 is inby and in surface 3 it is outby.

Results presented above show that the maximum ground strains expected on a stream bed can be mitigated as a function of the relative location of the stream axis to the rib of the excavation.

2.3.2. Case study 2: the effect of horizontal strain on groundwater flow

To evaluate the effect of mining-induced strains on the hydrogeological system, a conceptual model containing a subsurface aquifer overlying an active longwall panel was developed using MODFLOW. With an excavation height of 2 m, the caving zone, as defined by Peng and Chiang, extends up to 20 m (up to 10 times the seam thickness) from the coal seam into the overburden strata

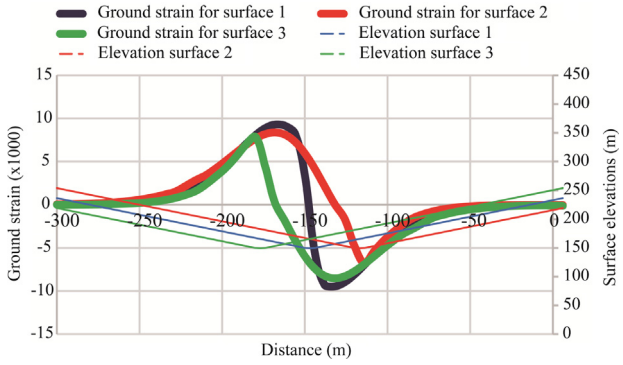

Fig. 10. Ground strain profiles on a transverse line above a longwall panel with respect to varying stream bed locations.

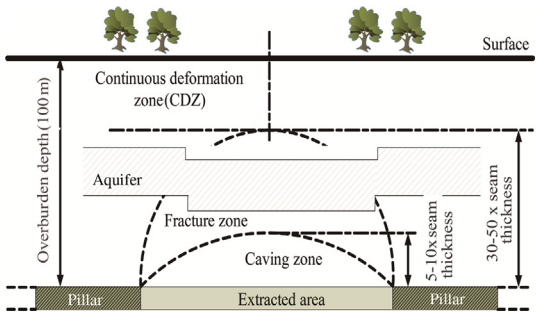

Fig. 11. Aquifer location with respect to the fracture and caving zones [26].

[26]. As shown in Fig. 11, the subsurface aquifer is therefore located in the fractured zone (30–50 times the seam thickness). In order to evaluate the effect of mining-induced strains on groundwater flow conditions, pre- and post-mining groundwater models were developed simulating water flows through a simplistic three-dimensional block 1380 m wide (138 elements), 2000 m long (200 elements) and 100 m deep. Each model was developed such that it simulates water flow over a year, given 12 (time) stress periods each spanning 30 days.

Each model is comprised of four layers (Fig. 12) corresponding to four stratified geological formations. Their respective geometric as well as pre- and post-mining hydraulic properties are given in Table 3. Layer 1 was defined as an unconfined shale formation 40 m thick with a hydraulic conductivity of 0.0864 m/day (1.00E−06 m/s) in both the horizontal and vertical directions as interpreted from the literature. Layer 2 was defined as an unconfined aquifer (sandstone) with variable transmissivity layer type that is 20 m thick with a pre-mining vertical and horizontal hydraulic conductivity of 8.64 m/day (1.00E−04 m/s) and a post-mining vertical and horizontal conductivity of 86.4 m/day (1.00E−03 m/s) correlating to a strain value of 0.01723. Since Layer 2 represents an unconfined water-bearing sandstone aquifer, an initial head of 60 m was defined for Layer 2 while Layers 1, 3, and 4 of the model were defined with initial heads of zero.

Layer 3 was defined as a confined shale formation 40 m thick with a pre-mining vertical and horizontal conductivity of 0.0866 m/day (1.00E−06 m/s) and a post-mining vertical and horizontal conductivity of 0.864 m/day (1.00E−05 m/s), correlating to a strain value of 0.01723. Layer 4 was defined as a confined coal seam which is 2 m thick with a pre-mining vertical and horizontal conductivity of 0.864 m/day (1.00E−05 m/s) and a post-mining vertical and horizontal conductivity of 8.64 m/day (1.00E−04 m/s).

As MODFLOW operates with differences in head and/or elevation, an arbitrary datum of zero elevation was assumed to lie at the top of Layer 4 such that the cumulative thickness of layers 1–3 represents the overburden depth over the coal seam. All layers within this model were defined with default values for specific storage (0.0001 m^{-1}) and specific yield (0.25). Post-mining hydraulic conductivities were defined in the areas of mining disturbance, and their magnitude was estimated based on horizontal strains

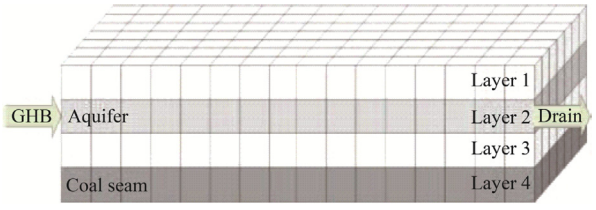

Fig. 12. Pre-mining groundwater model (not to scale).

Table 3
MODFLOW input parameters and change in mining-induced horizontal strain.

Layer	Thickness (m)	Hydraulic head (m)	Pre-mining hydraulic conductivity		Change in Horizontal strain	Post-mining hydraulic conductivity		Change ratio in hydraulic conductivity	Comment
			(m/s)	(m/day)		(m/s)	(m/day)		
Layer 1	40	0	1.00E−06	0.0864	0	1.00E−06	0.0864	1	Overburden assumed impermeable
Layer 2	20	60	1.00E−04	8.6400	0.0172	1.00E−03	86.4000	10	Aquifer assumed unconfined
Layer 3	40	0	1.00E−06	0.0864	0.0172	1.00E−05	0.8640	10	Overburden assumed impermeable
Layer 4	2	0	1.00E−05	0.8640	0.0172	1.00E−04	8.6400	10	Coal seam

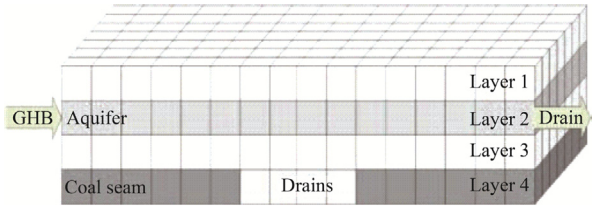

Fig. 13. Post-mining groundwater model (not to scale).

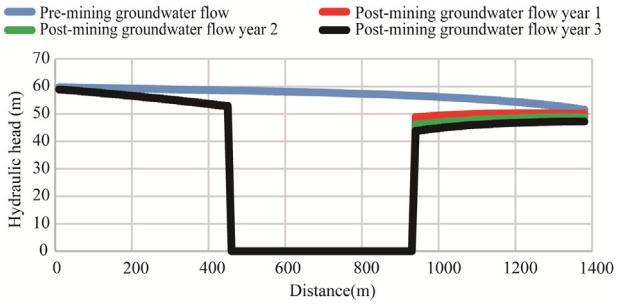

Fig. 14. Effect of mining on groundwater flow through an aquifer.

determined by the influence function method of the SDPS package (Table 3). Recharge of the groundwater system due to precipitation was not considered in this model, nor was the removal of water from the system with respect to plant transpiration or evaporation.

As shown in Figs. 12 and 13, two boundary conditions were applied to the sandstone aquifer (Layer 2) for both pre- and post-mining groundwater models. A general head boundary with a conductance of 34.25 m^2/day (3.96E−04 m^2/s) was defined on the eastern edge of the aquifer, while a drain with a conductance of 34.25 m^2/day (3.96E−04 m^2/s) was defined along the western boundary of the aquifer. In defining these boundary conditions, water flow through the aquifer can be simulated by the model. In order to simulate the post-mining flow of groundwater into the mine with respect to the excavation of coal by the longwall, drains with a conductance of 0.5 m^2/day (6.00E−06 m^2/s) were defined for element 46–92 in Layer 4, as shown in Fig. 13.

3. Results and discussion

Comparing the MODFLOW results of the pre- and post-mining head of the aquifer for this hypothetical case study, one is able to evaluate the impact of mining-induced strains on groundwater conditions. Before mining occurs, the water level within the aquifer gradually decreases from an initial head of 60 m to a head of 51 m across the simulated area, as represented by the blue line shown in the cross-section presented in Fig. 14. Note that unconfined aquifers may show either a head decrease or a constant head along a specific length.

These results are then compared to that of the post-mining water levels within the aquifer. In these cases, groundwater flow simulations start after all mining has been completed, while pumping (water loss) at mine level continues. Here, one finds that the increase in hydraulic conductivity with respect to mining-induced strains in the overburden results in the dewatering of the aquifer in the area directly overlaying the mined-out panel. The simulation is performed for periods of one, two, and three years for a constant water removal rate.

As shown in Fig. 14, for all simulated time periods, the hydraulic head within the aquifer gradually decreases as it approaches the longwall panel. In the overburden area directly above the longwall panel, water within the aquifer is lost to the lower geologic layers due to the mining-induced increase in hydraulic conductivity for years one, two, and three. Similar results were found by Guo et al., while monitoring the water levels of piezometers located above a longwall district in the Pittsbugh #8 coal seam [27]. From the data collected from monitored piezometers located over the mined area the authors found that the water levels decreased to immeasurable levels indicating a dry well. The water levels of piezometers outside the zone of mining induced overburden impacts mined area remained relatively constant during the entirety of the mining process encountering only slight water loss before recharging to its pre-mining water level [27].

On the eastern side of the modeled longwall panel, in the area of non-impacted overburden material, the hydraulic head gradually decreases from the eastern boundary to the eastern edge of the gob panel as groundwater flows into the mine workings. As simulation time increases to years two and three, the water level at the eastern side tends to decrease as pumping continues and there is no recharge applied to the model. These graphs are indicative of aquifer behavior since simulation results depend on model assumptions regarding formation permeability and storativity, as well water input and outputs. Furthermore, once mining operations cease and aquifer water is not removed from the system, simulations show that the aquifer will recover to its original levels. In addition, Guo et al. observed that the piezometer outside the affected overburden area not only stabilized to its pre-mining water level, but over the course of two years water levels were observed to be higher than the pre-mining levels [27]. This is similar to observed downstream waters level recovery in surface streams [28]. Mining-induced surface cracks can potentially drain streams in areas above underground longwall panels. The water is diverted through these cracks into subsurface aquifers. Given time, these aquifers will become full and force water back to the surface downstream from where the original water loss occurred.

4. Summary and conclusions

Increases in environmental scrutiny from community and regulatory agencies have created significant obstacles for mining companies to obtain mining and reclamation permits [16]. Currently, the Office of Surface Mining Reclamation and Enforcement (OSMRE) is looking to impose new regulations in 2016 for the pro-

tection of streams and groundwater from adverse impacts of surface and underground mining operations (80 FR 44435), which could possibly sterilize large amounts of coal reserves.

This paper examines the implementation of a general methodology for operations personnel to evaluate mining-induced impacts on surface and subsurface bodies of water. Through the utilization of the influence function formulation in SDPS, one is able to predict mining-induced ground deformations at any point in the three-dimensional space and, therefore, at any point along the surface topography or at any elevation within the overburden strata.

A hypothetical case study simulating a stream in a hill/valley system is utilized for calculating the distribution of ground strain along linear surface water bodies under simple geometrical considerations. Calculations indicate that the maximum ground strains expected on a stream bed can be mitigated as a function of the relative location of the stream axis to the rib of the excavation as well as the orientation of the stream with respect to the longwall panel. More work needs to be done for quantifying the effect of stream orientation, overburden topography to panel orientation and edge effect offset.

A second hypothetical case study was investigated where subsurface strain outputs from SDPS were used in the assessment of mining-induced changes to the hydraulic conductivity of the overburden strata and, therefore, changes to the hydrogeological system above a high-extraction area. Results show that in overburden areas disturbed by underground mining operations, groundwater levels at an aquifer will gradually decrease while water is removed from the underground working through pumping or other means. When water outflows at mine level cease then the aquifer present in the overburden will rebound. These results were further compared to the field work of Guo et al., which indicated the similar outcomes to those obtained by the MODFLOW model [27]. While the results of the model presented in this paper point to a promising methodology for the evaluation of mining-induced impacts on subsurface bodies of water, further research is needed for validating hydraulic conductivity changes and water head distribution above high-extraction areas.

Acknowledgments

This study was sponsored by the Appalachian Research Initiative for Environmental Science (ARIES). The views, opinions and recommendations expressed in this paper are solely those of the authors and do not imply any endorsement by ARIES employees or other ARIES-affiliated researchers. The authors would also like to thank the reviewers of this paper for their diligence in technically reviewing this work.

References

[1] Peng SS. Coal mine ground control. 3rd ed. Morgantown, West Virginia: West Virginia University; 2008.
[2] Singh MM. Mine subsidence, section 10.6. SME mining engineering handbook. Colorado: Littleton: SME; 1992.
[3] Booth CJ. Strata-movement concepts and the hydrogeological impact of underground coal mining. Ground Water 1986;24(4):507–15.
[4] Bian ZF, Inyang HI, Daniels JL, Frank OT, Struthers S. Environmental issues from coal mining and their solutions. Mining Sci Technol 2009;20(2):215–23.
[5] McNally G, Evans R. Impacts of longwall mining on surface water and ground water, southern coalfield NSW. Australia: NSW Department of Environment and Climate Change. Water Cooperative Research Center; 2007.
[6] Iannacchione A, Tonsor S, Witkowski M, Benner J, Hale A, Shendge M. The effects of subsidence resulting from underground bituminous coal mining on surface structures and features and on water resources: 3rd ACT 54 five-year report. University of Pittsburg; 2010.
[7] Waddington AA, Kay DR. Research into the impacts of mine subsidence on the strata and hydrology of river valleys and development of management guidelines for undermining cliffs, gorges, and river systems–stage 2. Brisbane, Australia: Australian Coal Association Research Program (ACARP). ACARP Research Report Project C9067; 2002.
[8] Karacan CÖ, Goodman G. Hydraulic conductivity changes and influencing factors in longwall overburden determined by slug tests in gob gas ventholes. Int J Rock Mech Min Sci 2009;46(7):1162–74.
[9] Karmis M, Agioutantis Z, Andrews K. Enhancing mine subsidence prediction and control methodologies. In: Proceedings, 27th international conference on ground control in mining, Morgantown, West Virginia. p. 131–6.
[10] McDonald MG, Harbaugh AW. A modular three-dimensional finite-differences groundwater flow model. In: Techniques of water-resources investigations. Reston, Virginia: US Geological Survey; 1988.
[11] Agioutantis Z, Newman C, Böde Jimenez Leon G, Karmis M. Minimizing impacts on streams due to underground mining by predicting surface ground movements. Min Eng 2016;68(3):28–37.
[12] Agioutantis Z, Karmis M, Kirby L. Application of subsidence prediction methodologies for sizing barrier pillars for stream protection in Appalachia. In: Craynon JR, editor. Proceedings, symposium on environmental considerations in energy production. Charleston, West Virginia: SME; 2013. p. 319–35.
[13] Agioutantis Z, Karmis M. Recent developments on surface ground strain calculations due to underground mining in Appalachia. In: Proceedings, 32nd international conference on ground control in mining, Morgantown, West Virginia. p. 214–9.
[14] Deck O, Harlaka A. Study of soil-structure interaction phenomena within mining subsidence areas, post-mining 2008, February 6–8, Nancy, France.
[15] Liu J, Elsworth D, Matetic RJ. Evaluation of the post-mining groundwater regime following longwall mining. Hydrol Process 1997;11(15):1945–61.
[16] Booth CJ. Groundwater as an environmental constraint of longwall coal mining. Mater Geoenviron 2006;50(1):49–52.
[17] Hawkins J, Smoyer JJ. Hydrologic impacts of multiple-seam underground and surface mining: a northern Appalachia example. Mine Water Environ 2011;30(4):263–73.
[18] Karacan CÖ. Prediction of porosity and permeability of caved zone in longwall gobs. Transp Porous Media 2010;82(2):13–439.
[19] Zaidel J, Markham B, Bleiker D. Simulating seepage into mine shafts and tunnels with MODFLOW. Ground Water 2010;48(3):390–400.
[20] Matetic RJ, Liu J, Elsworth D. Modeling the effects of longwall mining on the ground water system. USBM RI 9561. Bureau of Mines, Pittsburgh, Pa; 1995.
[21] Li Y, Peng SS, Zhang J. Impact of longwall mining on groundwater above the longwall panel in shallow coal seams. J Rock Mech Geotech Eng 2015;7(3):298–305.
[22] Toran L, Bradbury KR. Groundwater flow model of drawdown and recovery near an underground mine. Ground Water 1988;26(6):724–33.
[23] McCoy KJ, Donovan JJ, Leavitt BR. Estimation of hydraulic conductivity of coal mine barriers, Pittsburgh coal, Northern West Virginia, 1992-2000. In: Proceedings, 25th West Virginia surface mine drainage task force, Lexington, Kentucky. p. 1218–26.
[24] Rapantova N, Grmela A, Vojtek D, Halir J, Michalek B. Ground water flow modeling applications in mining hydrogeology. Mine Water Environ 2007;26(4):264–70.
[25] Ouyang Z, Elsworth D. Evaluation of groundwater flow into mined panels. Int J Rock Mech Min Sci 1993;30(2):71–9.
[26] Peng SS, Chiang HS. Longwall mining. New York: Wiley; 1984.
[27] Guo WB, Zou YF, Hou QL. Fractured zone height of longwall mining and its effects on the overburden aquifers. Int J Mining Sci Technol 2012;22(5):603–6.
[28] Tieman G, Rauch H. Study of dewatering effects at a longwall mine in northern West Virginia. In: 3rd Workshop on surface subsidence due to underground mining, West Virginia: Morgantown.